# Transcranial direct-current stimulation modulates synaptic mechanisms involved in associative learning in behaving rabbits

Javier Márquez-Ruiz[a], Rocío Leal-Campanario[a], Raudel Sánchez-Campusano[a], Behnam Molaee-Ardekani[b,c], Fabrice Wendling[b,c], Pedro C. Miranda[d], Giulio Ruffini[e], Agnès Gruart[a], and José María Delgado-García[a,1]

[a]Division of Neurosciences, Pablo de Olavide University, 41013 Seville, Spain; [b]Institut National de la Santé et de la Recherche Médicale U642, Rennes F-35000, France; [c]Laboratoire Traitement du Signal et de L'Image, Université de Rennes 1, Rennes F-35000, France; [d]Neuroelectrics, 08022 Barcelona, Spain; and [e]Starlab Barcelona SL, 08022 Barcelona, Spain

Edited* by Ivan Izquierdo, Centro de Memoria, Pontifical Catholic University of Rio Grande do Sul, Porto Alegre, Brazil, and approved March 20, 2012 (received for review December 21, 2011)

**Transcranial direct-current stimulation (tDCS) is a noninvasive brain stimulation technique that has been successfully applied for modulation of cortical excitability. tDCS is capable of inducing changes in neuronal membrane potentials in a polarity-dependent manner. When tDCS is of sufficient length, synaptically driven after-effects are induced. The mechanisms underlying these after-effects are largely unknown, and there is a compelling need for animal models to test the immediate effects and after-effects induced by tDCS in different cortical areas and evaluate the implications in complex cerebral processes. Here we show in behaving rabbits that tDCS applied over the somatosensory cortex modulates cortical processes consequent to localized stimulation of the whisker pad or of the corresponding area of the ventroposterior medial (VPM) thalamic nucleus. With longer stimulation periods, poststimulation effects were observed in the somatosensory cortex only after cathodal tDCS. Consistent with the polarity-specific effects, the acquisition of classical eyeblink conditioning was potentiated or depressed by the simultaneous application of anodal or cathodal tDCS, respectively, when stimulation of the whisker pad was used as conditioned stimulus, suggesting that tDCS modulates the sensory perception process necessary for associative learning. We also studied the putative mechanisms underlying immediate effects and after-effects of tDCS observed in the somatosensory cortex. Results when pairs of pulses applied to the thalamic VPM nucleus (mediating sensory input) during anodal and cathodal tDCS suggest that tDCS modifies thalamocortical synapses at presynaptic sites. Finally, we show that blocking the activation of adenosine A1 receptors prevents the long-term depression (LTD) evoked in the somatosensory cortex after cathodal tDCS.**

The effects of weak direct-current (DC) stimulation on the excitability of the central nervous system were reported decades ago. Invasive stimulation in acute animals demonstrated that intracortical or epidural application of weak DC induces polarity-specific changes in the neuronal excitability of motor (1, 2), visual (1), and somatosensory (3) cortices. Interestingly, these changes persist for several minutes after the DC stimulus offset (3), sharing some molecular mechanisms with the classical long-term plasticity. In this regard, it has been demonstrated that anodal DC stimulation applied on the rat sensorimotor cortex modifies adenosine-elicited accumulation of cAMP (4), inducing an increase of protein kinase C and calcium levels (5, 6). tDCS has been successfully applied for modulation of cortical excitability in humans (7–11), and interest is growing in the use of this technique as a noninvasive tool for basic and clinical research in various neurologic pathologies, including chronic pain, stroke, and depression (12–15). Little is known about the molecular and/or cellular mechanisms underlying the neuromodulatory after-effects of tDCS, however. For this reason, new experimental models are needed for testing the effects of applying tDCS to different cortical areas in alert behaving animals, specifically to demonstrate the effectiveness of tDCS on the modulation of sensory perception involved in complex cortical processes, such as the acquisition of an associative learning task, as well as the way in which tDCS affects the activity of intrinsic cortical circuits.

## Results

In a first series of experiments, we tested whether simultaneous tDCS applied to the somatosensory cortex could modify the characteristics of local field potentials (LFPs) evoked in the vibrissa S1 area of alert behaving animals by air puff stimulation of the contralateral whisker pad (Fig. 1*A*). Whisker stimulation evoked a short-latency (mean ± SEM, 15.4 ± 2.5 ms; $n = 103$) negative LFP (N1, Fig. 1*B*), followed by late positive and negative components (Fig. S1*A*) and then a smaller LFP evoked at the end of the air puff. The amplitude of air puff-evoked LFPs depended on the stimulus intensity and on the recording site across the somatosensory cortical layers (Fig. S1 *A* and *B*).

The N1 component of the LFP was amplified by the simultaneous presence of an anodal tDCS and was reduced by cathodal tDCS (Fig. 1*B*). Indeed, the N1 component was significantly increased in both amplitude (up to a mean maximum of 153 ± 16.2%; $n = 5$; $P \leq 0.05$, one-way ANOVA) and area (up to a mean maximum of 247.1 ± 82.8%, $n = 5$, $P \leq 0.05$, one-way ANOVA) in response to anodal tDCS (from 0.5 mA to 2 mA; Fig. 1*C*). In contrast, cathodal tDCS (from −0.5 mA to −2 mA) decreased the amplitude (by up to a mean maximum of 63.9 ± 13.1%; $n = 5$) and area (by 61.3 ± 16.8%; $n = 5$) of the N1 component compared with N1 values collected from controls and during the presentation of anodal tDCS (Fig. 1*C*). Thus, concurrent tDCS applied to the somatosensory cortex was capable of increasing or decreasing the amplitude and area of LFPs evoked by the simultaneous air puff stimulation of the whisker pad. Moreover, tDCS had a persistent poststimulus effect; the inhibitory effect of 1 mA of cathodal tDCS on N1 amplitude was significantly [$F_{(7,28,760)} = 16.943$; $P < 0.001$, repeated-measures ANOVA] evident for up to 30 min after the end of the DC stimulation (Fig. 1*D*). Confirming previous results reported in humans (16), these experiments show that tDCS can modify the functional properties of LFPs evoked in the somatosensory area

Author contributions: J.M.-R., R.L.-C., G.R., A.G., and J.M.D.-G. designed research; J.M.-R., R.L.-C., A.G., and J.M.D.-G. performed research; R.S.-C., B.M.-A., F.W., and P.C.M. contributed new reagents/analytic tools; R.S.-C., B.M.-A., and P.C.M. analyzed data; and J.M.-R., G.R., A.G., and J.M.D.-G. wrote the paper.

The authors declare no conflict of interest.

*This Direct Submission article had a prearranged editor.

Freely available online through the PNAS open access option.

[1]To whom correspondence should be addressed. E-mail: jmdelgar@upo.es.

This article contains supporting information online at www.pnas.org/lookup/suppl/doi:10.1073/pnas.1121147109/-/DCSupplemental.

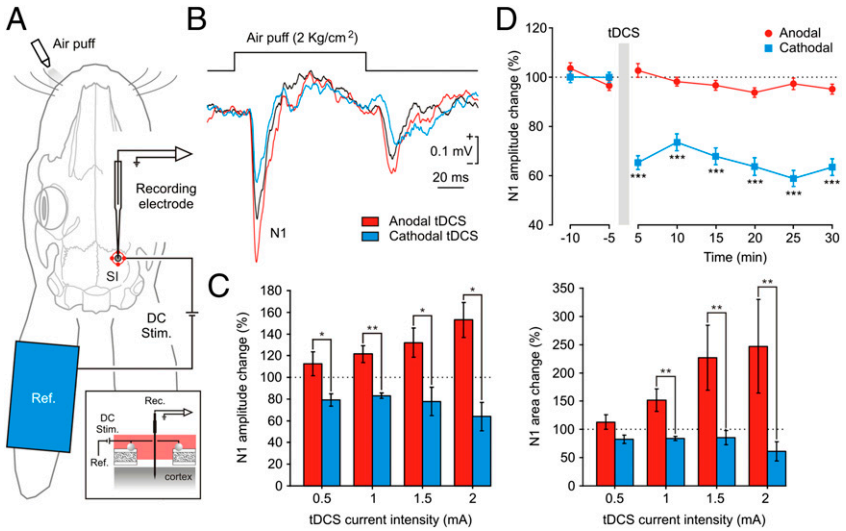


**Fig. 1.** Effects of tDCS on LFP evoked in the vibrissa S1 area of the somatosensory cortex. (*A*) Experimental design illustrating the electrode locations for tDCS and the recording micropipette. Both anodal and cathodal tDCS currents were applied between the active (red circles) and the reference (Ref.) electrodes. Air puff stimulation of the contralateral whisker pad is shown as well. (*Inset*) Schematic sagittal view of the recording site at which LFP corresponding to vibrissa was mapped, the tungsten electrode (Rec.) was attached to the skull, and the window was cut in the parietal bone and subsequently covered with dental cement. (*B*) Representative examples of LFP evoked in the vibrissa S1 cortex by air puff stimulation of the contralateral whisker pad in control situation (black recording) and during the application of anodal tDCS (red recording) or cathodal tDCS (blue recording). (*C*) Changes in amplitude (*Left*) and area (*Right*) of the N1 component (indicated in *B*) of air puff-evoked LFP in the presence of anodal currents (red histograms) or cathodal currents (blue histograms) at increasing intensities. $n = 5$. $^{*}P < 0.005$; $^{**}P < 0.01$, one-way ANOVA. (*D*) After-effects of tDCS. LFP evolution after anodal tDCS (red) and cathodal tDCS (blue). $^{***}P < 0.001$, repeated-measures ANOVA. Error bars represent SEM.

by natural stimulation of facial mechanoreceptors, including a noticeable poststimulus effect on cathodal currents.

In a second series of experiments, we tested whether simultaneous tDCS could also modulate the acquisition of a well-known model of associative learning, the classical conditioning of eyelid responses, using stimulation of the whisker pad as a conditioned stimulus (CS). A previous study indicated that specific areas of the somatosensory cortex are activated during this type of associative learning, depending on the skin site of the CS presentation (17). As in that study, we used a train of pulses (100 ms, 200 Hz) presented to the whisker pad as CS, followed 250 ms later by an air puff presented to the ipsilateral cornea as an unconditioned stimulus (US). Two habituation sessions (H1 and H2, when the CS was presented alone) and 10 conditioning sessions (C1–C10, with paired CS–US presentation) were carried out. Each conditioning session consisted of 66 trials (6 series of 11 trials each) separated at random by intervals of 50–70 s. Of the 66 trials, 6 were test trials in which the CS was presented alone (Fig. 2*A*). Fig. 2*B* presents representative samples of classically conditioned eyelid responses collected from C2 and C8 in the control situation (conditioning series 1, traces in black) and during anodal (red trace in C2) and cathodal (blue trace in C8) stimulation. In agreement with previous reports (18), control animals reached asymptotic values (>80% of conditioned responses per session) for their learning curves by C3 or C4 (Fig. 2*C*). The experimental group was presented with three blocks of anodal tDCS (≤1 mA) applied over the right somatosensory cortex, contralateral to the CS–US, during conditioning series 2, 4, and 6 of C2 (Fig. 2*C*). The presence of concurrent anodal tDCS during C2 was associated with a significant increase in the percentage of conditioned responses [59.9 ± 11.2 for controls vs. 95.6 ± 3.5 for stimulated animals; $F_{(1,5,4)} = 9.279$; $P < 0.05$, one-way ANOVA] (Fig. 2*C*). The experimental group also was presented with three blocks of cathodal tDCS (≤−1 mA) during conditioning series 2, 4, and 6 of C8 (Fig. 2*A*). In this case, stimulated animals showed a significantly lower percentage of conditioned responses compared with the control group [49.3 ± 10.5 vs. 90.5 ± 1.7; $F_{(1,5,4)} = 14.934$; $P < 0.05$, one-way ANOVA]. Thus, by using tDCS to decrease or enhance sensory perception process, we were able to modulate the animals' ability to acquire a typical associative learning test, such as classical eyeblink conditioning (19). An intrasession analysis of classical conditioning evolution during sessions in which anodal (C2) or cathodal (C8) tDCS was presented to the somatosensory cortex of the experimental group is illustrated in Fig. 2*D*. As shown, concurrent anodal tDCS increased the rate of conditioned responses across the session, whereas cathodal tDCS decreased this rate during the stimulation session as well as thereafter. This findings support the idea that tDCS modifies the associative strength of cortical circuits involved in associative learning (20, 21).

We carried out two additional series of experiments to examine the putative mechanisms underlying the short- and/or long-term effects of tDCS on the somatosensory cortex. In the first of these experiments, we performed a paired-pulse test in two animals to determine whether presynaptic processes involved in the thalamocortical sensory input could be affected by simultaneous anodal or cathodal tDCS. Fig. 3*A* illustrates monosynaptic (>6 ms) field excitatory postsynaptic potentials (fEPSPs) evoked at the vibrissa S1 cortex by pairs of pulses (at 20-ms intervals) applied to the ipsilateral VPM nucleus of the thalamus (22). As shown in Fig. 3*B*, the amplitude (in millivolts) of fEPSPs evoked in the somatosensory cortex by the first pulse increased steadily with current strength until it reached asymptotic values. In contrast, fEPSPs evoked by the second pulse increased roughly in parallel with the fEPSPs evoked by the first pulse (but with larger values) up to a certain stimulus intensity, after which the fEPSP slopes evoked by the second pulse were smaller than those evoked by the first pulse. In fact, the second/first paired-pulse ratio decreased progressively from facilitation to depression, with an inflection point at ~2.2 mA (Fig. 3*C*). The paired-pulse test indicated that thalamocortical synapses present a paired-pulse facilitation at low intensities that is reversed to paired-pulse depression at higher intensities. The simultaneous presence of anodal or cathodal tDCS modulated, and even reversed, the paired-pulse relationship at either low (Fig. 3*D*) or

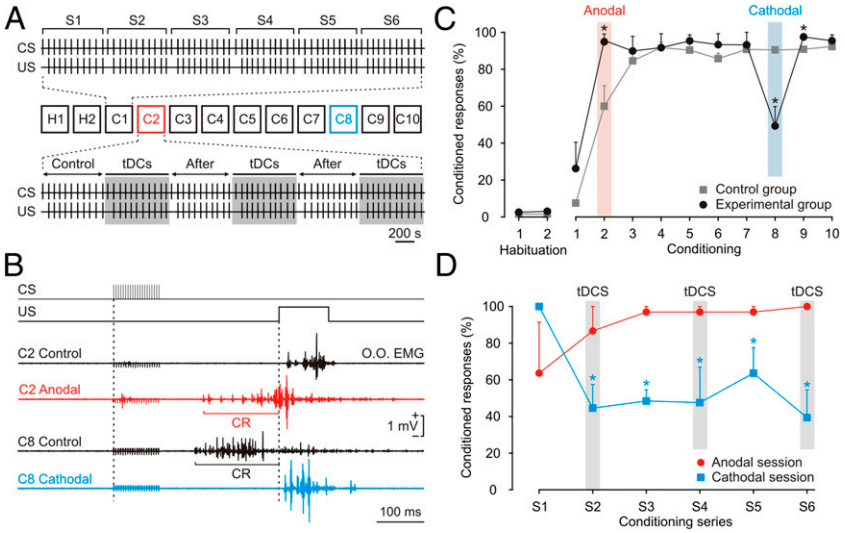


**Fig. 2.** Effects of tDCS on classical eyeblink conditioning using a trace paradigm. (*A*) Experimental design. Two habituation sessions (H1 and H2) and 10 conditioning sessions (C1–C10) were carried out. Conditioning sessions consisted of 66 trials (6 series of 11 trials each) separated at random by intervals of 50–70 s. Of the 66 trials, 6 were test trials in which the CS was presented alone. Anodal tDCS was presented during series 2, 4, and 6 of C2 (in red), and cathodal tDCS was presented in these same series during C8 (in blue). (*B*) The conditioning paradigm (CS and US presentations) and representative orbicularis oculi electromyographic (O.O. EMG) recordings collected from the same animal during the C2 session from a control series (conditioning series 1, traces in black) and during anodal stimulation (trace in red) and during the C8 session from a control series and during cathodal stimulation (trace in blue). The presence of conditioned responses (CR) is indicated for the anodal-stimulated animal during the C2 session and for the control animal during the C8 session. (*C*) Evolution of learning curves for a control group of animals (gray squares and line) and the experimental group. The experimental group received anodal tDCS during C2 and cathodal tDCS during C8. $n = 6$. $P < 0.05$, one-way ANOVA. (*D*) Evolution of the percentage of conditioned responses during sessions with anodal tDCS (C2, in red) and cathodal tDCS (C8, in blue). Series during which tDCS was applied (S2, S4, and S6) are indicated by a gray bar. $P < 0.05$, Mann-Whitney test. Error bars represent SEM.

high (Fig. 3*E*) stimulation intensities, suggesting that tDCS modifies thalamocortical synapses at presynaptic sites (23).

In the second series of additional experiments, we examined the synaptic mechanisms underlying the long-lasting depressant effects on cortical activity produced by cathodal tDCS. Based on previous studies of the molecular processes underlying LTD (24, 25), we investigated the effect of the selective A1 adenosine receptor antagonist 8-cyclopentyl-1,3-dipropylxanthine (DPCPX) when injected at the cortical recording site. Local microinjection of DPCPX significantly diminished the LTD induced after cathodal tDCS compared with vehicle controls ($n = 3$; $P < 0.001$, one-way ANOVA) (Fig. 3*F*).

## Discussion

This study demonstrates that associative learning processes can be modulated by tDCS applied over the somatosensory cortex, and contributes to our understanding of the neural mechanisms involved in short-term and long-lasting tDCS-induced effects. Although previous in vitro (26–28) and acute (1–3, 29, 30) animal studies have demonstrated the modulatory effects of DC on cortical excitability, until now no direct evidence of the effects of tDCS based on cortical recordings of electrical activity in alert animals has been reported. And although behaving animals have been successfully used for the study of different tDCS implications in basic (31–33) and clinical (34–36) aspects, the animal model presented here allows the combination of tDCS application in alert animals with invasive recording of cortical electrical activity.

We report here that intracortical recording of cortical sensory LFP during simultaneous tDCS shows an increase or decrease in the amplitude and area of the main field potential components, depending on the anodal or cathodal polarity of the applied current. This short-term effect corresponds to the effects reported in the motor cortex based on measurements of motor evoked potentials in humans (7, 37–40) and in anesthetized animals (29). Although the complete neurophysiological characterization of short-term effects is difficult due to the tDCS-induced artifacts in electrophysiological recordings, the behavioral changes observed during tDCS application point to the same general polarity-specific effects when applied to somatosensory (16, 41) and visual (42, 43) cortices. The changes in sensory LFPs or fEPSPs in response to whisker or VPM nucleus stimulation during tDCS reported here suggest a modification in the number of neurons recruited by the same stimulus, with consequent reinforcement or attenuation of the subjective perception of the stimulus.

To test whether sensory thalamic afferent signals can be modified by simultaneous tDCS, we used a paired-pulse test, applying stimulation at the thalamic VPM nucleus and recording the evoked LFPs in the somatosensory cortex (22). The paired-pulse test is commonly used to highlight presynaptic effects on neurotransmitter release (23). We found that the simultaneous presence of anodal or cathodal tDCS modulates the paired-pulse relationship, suggesting that tDCS modifies thalamocortical synapses at presynaptic sites. Our findings do not exclude the possibility of additional postsynaptic modifications, however. Thus, changes in the LFPs induced by whisker stimulation during tDCS seem to be the result of direct changes in the membrane potential of cortical neurons, together with changes in the neurotransmitter release of thalamocortical sensory afferents.

Only cathodal tDCS was able to induce significant poststimulus changes (i.e., decreased amplitude and area of the N1 component) in the recorded LFPs, which persisted for up to 30 min. In contrast, no changes were observed after anodal tDCS. Similar results have been reported in sensory evoked potentials after tDCS application over the human somatosensory cortex. Dieckhöfer et al. (11) reported a significant reduction in the N20 component after cathodal tDCS, but no changes after anodal tDCS. Similarly, in another study, pain perception and the amplitude of laser-evoked potentials were decreased after cathodal tDCS over the somatosensory cortex in humans, whereas no changes were observed after anodal tDCS (44).

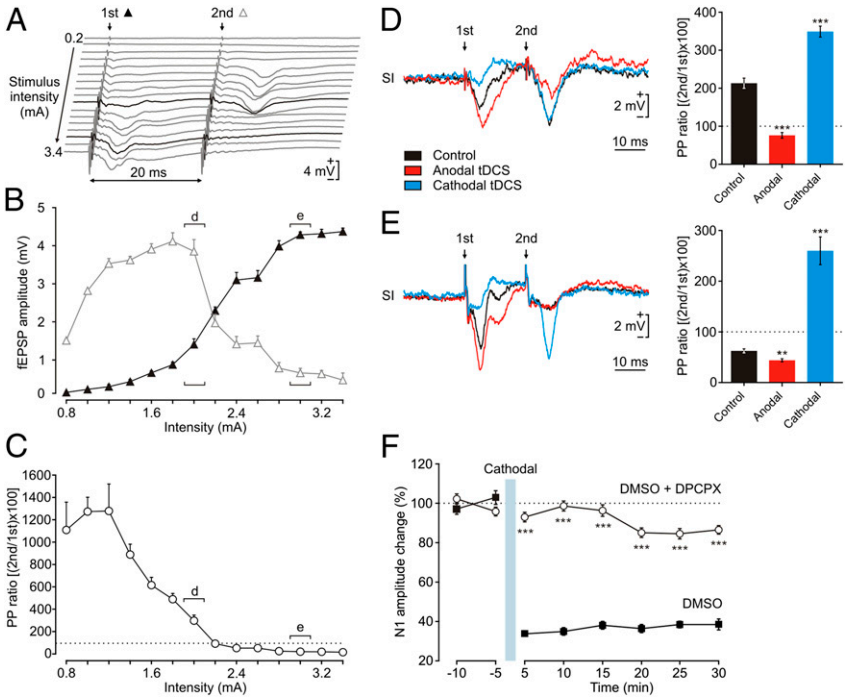


**Fig. 3.** Synaptic mechanisms involved in effects of tDCS on cerebral cortical circuits. (*A*) fEPSPs evoked in the somatosensory cortex by pairs of pulses (at 20-ms intervals) presented to the ipsilateral thalamic VPM nucleus at increasing intensities (0.2–3.4 mA). (*B*) Changes in fEPSP amplitude evoked by the first pulse (black triangles and line) and the second pulse (white triangles and gray line) illustrated in *A*, at increasing intensities. Paired-pulse (PP) facilitation was evoked at low intensities, whereas PP depression was evoked at high intensities. (*C*) The PP ratio was calculated as [(second fEPSP amplitude/first fEPSP amplitude) × 100]. (*D* and *E*) Effects of anodal tDCS (red recording) and cathodal tDCS (blue recording) on PP modulation of synaptic strength compared with controls (black recording). The PP intensity was 2 mA (*D*) or 3 mA (*E*). The bar graphs show changes in the PP ratio evoked by the three types of recordings. $^{**}P < 0.01$; $^{***}P < 0.001$, one-way ANOVA. (*F*) LFP evolution after cathodal tDCS in the presence of the selective A1 adenosine receptor antagonist DPCPX (open circles) or the injection of vehicle DMSO (squares in black). Pharmacologic antagonism of the adenosine A1 receptor significantly impaired LTD. $^{***}P < 0.001$, one-way ANOVA. Error bars represent SEM; some error bars are too small to be shown.

Previous studies performed in humans have attempted to elucidate neural mechanisms underlying the long-lasting effects observed after tDCS through the systemic administration of various drugs (45). Thus, NMDA receptors have been implicated in cathodal after-effects, and NMDA and $GABA_A$ receptors have been implicated in anodal after-effects (46, 47). Interestingly, experiments performed in rats support the results of human studies suggesting the participation of NMDA receptors in the process after anodal polarization (48). In addition, anodal DC stimulation applied over the rat sensorimotor cortex has been shown to modify adenosine-elicited accumulation of cAMP (4), inducing increases in protein kinase C and calcium levels (5, 6). Moreover, the involvement of adenosine A1 receptors in the LTD of cortical circuits has been reported recently (24, 49). Here we show that local microinjection of the adenosine A1 receptor antagonist DPCPX prevents the LTD evoked in the somatosensory cortex after cathodal tDCS. In contrast to other adenosine receptors, the adenosine A1 receptor suppresses neuronal activity by coupling with protein Gi to inhibit the adenylate cyclase–cAMP–protein kinase A signaling pathway (50). Previous reports adenosine-dependant increase in cAMP after anodal polarization (4–6), along with the evidence presented here implicating adenosine A1 receptor in cathodal after effects, point to a major role of adenosine in the modulation of cortical excitability induced by tDCS. In accordance with this, the selective pharmacologic manipulation of adenosine receptors during simultaneous tDCS may have important clinical applications.

Although the results reported here stress the importance of using animal models to study the immediate effects and after-effects of tDCS, some limitations of this experimental model must be taken into account. These limitations are associated mainly with differences between the electrodes used in rabbits and those used in clinical applications, hindering direct comparisons of current density and voltage distribution. According to the current distribution spherical head model (51), the maximum current density used in the rabbit brain was higher than that applied in humans during tDCS (Fig. S2). Nevertheless, no histopathological alterations were observed in the stimulated region (Fig. S3), confirming previous studies on the effects of tDCS in rats (31). Another limitation of this animal model is the simplicity of the rabbit cortical surface (i.e., the absence of circumvolutions) compared with the complex surface of the human cortex.

In conclusion, our results reported here support the findings of previous studies in humans regarding the effects of tDCS on the cerebral cortex, confirm the potential of this technique for modulating associative learning, and demonstrate the participation of adenosine A1 receptors in its selective actions on cortical circuits.

## Methods

**Animals.** Experiments were carried out on adult rabbits (New Zealand White albino; Isoquimen) weighing 2.3–2.7 kg on arrival. Before and after surgery, the animals were kept in one room but placed in independent cages. The animals were maintained on a 12-h light/12-h dark cycle with continuously controlled humidity (55 ± 5%) and temperature (21 ± 1 °C). All experimental procedures were carried out in accordance with European Union guidelines (2003/65/CE) and following Spanish regulations (RD 1201/2005) for the use of laboratory animals in chronic experiments. The experiments also were approved by the Ethics Committee of Pablo de Olavide University and by internal and external review boards of the Hyper Interaction Viability Experiments (HIVE) Project.

**Surgery.** Animals were anesthetized with a ketamine–xylazine mixture (Ketaminol 50 mg/mL, Rompun 20 mg/mL, atropine sulfate 0.5 mg/kg) at an

initial dosage of 0.85 mL/kg. Anesthesia was maintained by i.v. perfusion at a flow rate of 10 mg/kg/h. A first group of animals ($n$ = 7) was prepared for chronic recording of LFP in the somatosensory cortex in response to whisker or VPM stimulation in the presence of tDCS. Under aseptic conditions, a 2-mm-diameter hole was drilled through the parietal bone centered on the right S1 vibrissa area (row C: AP = −1.7 mm; L = 7 mm) (52). During drilling, the dura mater surface was protected by an inert plastic cover. To prepare a precisely focused active electrode (7), four silver ball stimulating electrodes (1 mm diameter; A-M Systems) were placed symmetrically above the skull 3 mm from the center of the drilled window (Fig. 1*A*). A silver electrode (1 mm in diameter) in contact with the dura mater was attached to the left parietal bone (AP = 10 mm; L = 6 mm) as a ground for LFP recordings. Two of these animals were also implanted with a bipolar stimulating electrode aimed at the right VPM nucleus (AP = 4.5 mm; L = 4.5 mm; D = 13.5 mm) (52) to measure the paired-pulse effect on fEPSP in the S1 cortex. A head-holding system, consisting of three bolts cemented to the skull perpendicular to the stereotaxic plane, was implanted. Stimulating electrodes were connected to a socket attached to the holding system.

A second group of animals ($n$ = 6) was prepared for classical eyeblink conditioning and simultaneous tDCS. These animals were implanted with recording bipolar hook electrodes in the left orbicularis oculi muscle. A pair of stimulating electrodes was implanted in the center of the whisker pad (row C, column 3). These electrodes were made of Teflon-coated stainless steel wire (A-M Systems) with an external diameter of 230 μm and a ∼1-mm bare tip. Following the same procedure described above, four silver ball stimulating electrodes (1 mm diameter; A-M Systems) were placed symmetrically above the skull 3 mm from the right S1 vibrissa area. A head-holding system was implanted, and stimulating and recording electrodes were connected to a socket attached to the holding system.

**Recording and Stimulation Procedures.** Recording sessions were started at 2 wk after surgery. Each animal was placed in a Perspex restrainer box designed to limit movement (18). The animal's head was fixed to the recording table with the head-holding system. In all animals, the first two sessions involved adapting the animal to the restrainer and the experimental conditions. For characterization of LFPs evoked in the S1 cortex during tDCS, a glass micropipette was inserted into S1 areas corresponding to the whiskers. The first recording sessions were used to map the receptor field of the contralateral whisker pad by air puff stimulation of the whiskers. Once the S1 cortex was mapped, the glass micropipette was replaced with a chronically implanted Parylene-C insulated tungsten microelectrode (0.5 MΩ resistance; A-M Systems). After placement in the proper recording site, the tungsten electrode was attached to the skull, and the hole in the parietal bone was covered with dental cement (Fig. 1*A*, *Inset*). LFPs were recorded using a Tektronix AM 502 differential amplifier with a bandwidth of 1 Hz to 10 kHz. In the conditioning sessions during eyeblink conditioning, electromyography (EMG) of the orbicularis oculi was recorded using an A-M Systems 3600 differential amplifier with a bandwidth of 1 Hz to 10 kHz. Air puffs directed at the whiskers or the eye during conditioning were applied through the opening of a plastic pipette (3 mm diameter) attached to a holder fixed to the recording table (air puff device from Biomedical Engineering). Electrical stimulation of the whisker pad and VPM nucleus was achieved across an isolation unit (Cibertec). Single and double cathodal square (100-μs pulses) and train (200 Hz) stimuli were delivered with a Cibertec CS-220 programmable stimulator.

**tDCS.** tDCS was delivered by a battery-driven World Precision Instruments A395 Linear Stimulus Isolator. In contrast to humans, in rabbits the skin covering the skull is highly movable with respect to the underlying bones. For this reason, tDCS was applied simultaneously to the four silver ball stimulating electrodes, with a saline-soaked sponge (35 $cm^2$ surface area) attached to the contralateral ear serving as a counterelectrode. To index changes in the somatosensory cortex during and after anodal and cathodal tDCS, LFPs evoked in response to contralateral whisker stimulation (air pulses, 100 ms, 2 $kg/cm^2$, delivered every 10 ± 3 s) were recorded before (control), during (immediate effects), and after (after-effects) tDCS presentation. To characterize immediate effects, 10-s pulses of anodal and cathodal tDCS of varying intensities (0.5, 1, 1.5, and 2 mA) were applied, separated by periods of nonstimulation. To determine the presence of after-effects, LFPs were acquired starting 20 min before and extending up to 40 min after anodal and cathodal tDCS (±1 mA, 20 min). According to the current distribution spherical head model (51), the maximum current density in the stimulated brain was 3.7 $A/m^2$ (Fig. S2). When necessary, sham stimulation involved the same electrode placement and protocols, except for tDCS duration (10 s instead of ∼10 min to the right somatosensory cortex during series 2, 4, and 6 of C2 and C8).

**Paired-Pulse Test.** For input/output curves, animals ($n$ = 2) were stimulated in the VPM nucleus at increasing intensities (0.8–3.4 mA). In addition, the effects of paired pulses were checked at various interstimulus intervals (10, 20, 40, 100, 200, and 500 ms) at intensities corresponding to 40% and 60% of the total required to evoke a saturating response. In all cases, the paired-pulse sequence of a given intensity was repeated five times at ≥30-s intervals, to avoid interference with slower short-term potentiation (augmentation) or depression processes (23). The interstimulus interval for the paired-pulse test during tDCS was set at 20 ms, to avoid interference with large/delayed field potential responses evoked in S1 after VPM stimulation (22).

**Classical Eyeblink Conditioning.** Classical conditioning of eyelid movements was achieved using a trace-conditioning paradigm. Animals were presented with a train (100 ms, 200 Hz) of electrical stimuli applied to the whisker pad as CS, followed 250 ms later by an air puff (100 ms, 3 $kg/cm^2$) presented to the cornea as US. The CS applied to the whisker pad was presented on the same side (left) as the US. Conditioning sessions consisted of 66 trials (6 series of 11 trials each) separated at random by intervals of 50–70 s. Of the 66 trials, 6 were test trials in which the CS was presented alone. Each conditioning session lasted for ∼80 min, and animals were trained for 12 successive days. The first two sessions consisted of the random presentation of CS alone (habituation sessions). As criteria, we considered a "conditioned response" the presence during the CS–US interval of EMG activity lasting >10 ms and initiated >50 ms after CS onset. In addition, the integrated EMG activity recorded during the CS–US interval had to be at least 1.2 times greater than the integrated EMG recorded immediately before CS presentation (18).

To characterize the impact of tDCS on classical conditioning, anodal and cathodal tDCS were presented to the experimental groups during C2 and C8, respectively. tDCS applied during a conditioning session consisted of anodal/cathodal current (anodal = 1–2 mA; cathodal = 1–2 mA; ∼30 min) presented during series 2, 4, and 6 within the same conditioning session. To avoid any sensory detection of tDCS, and as done in previous human studies (7, 8), sham stimulation in the control group involved the same electrode placement and conditioning protocol, except for tDCS duration (a total of 30 s instead of ∼30 min per conditioning session).

**Drug Microinjection.** After mapping of the S1 receptor field of the contralateral whisker pad, a tungsten microelectrode (A-M Systems) attached to a 24G guide tube was chronically implanted in the selected S1 area. The tip of the guide tube was set 2 mm above the tip of the recording electrode. During the experimental sessions, microinjections of the selective A1 adenosine receptor antagonist DPCPX (Sigma-Aldrich) were delivered by means of a 30G injection tube coupled to a 10-μL Hamilton syringe, which was advanced through the guide tube. The drug solution was injected constantly throughout the experiment at a rate of 0.1 μL/min. A total of 83 μg of DPCPX dissolved in 10 μL of DMSO was injected during the experiment, starting 15 min before cathodal tDCS.

**Histology.** At the end of the recording sessions, the animals were deeply anesthetized with sodium pentobarbital (50 mg/kg, i.p.) and perfused transcardially with 0.9% saline followed by 4% paraformaldehyde. The proper location of the whisker pad stimulating and EMG recording electrodes was then checked. To confirm the final location of the electrodes implanted in S1 and in the VPM, and to exclude DC-related tissue damage (Fig. S3), the brain was removed, cut into 50-μm slices, and processed for toluidine blue staining.

**Data Collection and Analysis.** Sensory LFP recordings, tDCS converted signals, unrectified EMG activity of the orbicularis oculi, and 1-V rectangular pulses corresponding to CS, US, air puff, and thalamus stimulations presented during the different experiments were stored digitally on a computer for quantitative offline analysis (Cambridge Electronic Design 1401*plus*). Data were sampled at 20 kHz for LFP recordings or 10 kHz for EMG recording, with an amplitude resolution of 12 bits. A computer program (SPIKE2; Cambridge Electronic Design) was used to quantify, with the aid of cursors, the peak amplitude and area of sensory LFP evoked in the S1 cortex and the onset latency, peak amplitude, and area of the rectified EMG activity of the orbicularis oculi muscle. Any LFPs evoked in the S1 cortex coincident with a tDCS-induced artifact were excluded from the analysis.

Statistical analyses were performed out using the SPSS package. The statistical significance of differences between groups was inferred by one-way ANOVA and repeated-measures ANOVA. The corresponding statistical

significance tests (i.e., $F_{[(m\text{-}1),\ (m\text{-}1)\ \times\ (n\text{-}1),\ (l\text{-}m)]}$ statistic) were reported, where *m*, *n*, and *l* indicate number of groups, number of animals, and number of observations, respectively. The nonparametric Mann–Whitney *U* test was applied for comparison when data did not permit an assumption of normality. Statistical significance was set at $P < 0.05$. Results are presented as mean ± SEM unless indicated otherwise.

**ACKNOWLEDGMENTS.** We thank Roger Churchill for his help with the manuscript and Claudia Ammann for her expert technical assistance. This work was funded by the European Union Seventh Framework Programme Future and Emerging Technologies (FET) Open Hyper Interaction Viability Experiments (HIVE) Project, which receives financial support from the FET Seventh Framework Program for Research of the European Commission, under FET Open Grant 222079.

1. Creutzfeldt OD, Fromm GH, Kapp H (1962) Influence of transcortical d-c currents on cortical neuronal activity. *Exp Neurol* 5:436–452.
2. Purpura DP, McMurtry JG (1965) Intracellular activities and evoked potential changes during polarization of motor cortex. *J Neurophysiol* 28:166–185.
3. Bindman LJ, Lippold OC, Redfearn JW (1962) Long-lasting changes in the level of the electrical activity of the cerebral cortex produced bypolarizing currents. *Nature* 196: 584–585.
4. Hattori Y, Moriwaki A, Hori Y (1990) Biphasic effects of polarizing current on adenosine-sensitive generation of cyclic AMP in rat cerebral cortex. *Neurosci Lett* 116: 320–324.
5. Islam N, Moriwaki A, Hattori Y, Hori Y (1994) Anodal polarization induces protein kinase C γ (PKCγ)-like immunoreactivity in the rat cerebral cortex. *Neurosci Res* 21: 169–172.
6. Islam N, Aftabuddin M, Moriwaki A, Hattori Y, Hori Y (1995) Increase in the calcium level following anodal polarization in the rat brain. *Brain Res* 684:206–208.
7. Nitsche MA, Paulus W (2000) Excitability changes induced in the human motor cortex by weak transcranial direct current stimulation. *J Physiol* 527:633–639.
8. Nitsche MA, et al. (2007) Shaping the effects of transcranial direct current stimulation of the human motor cortex. *J Neurophysiol* 97:3109–3117.
9. Antal A, Kincses TZ, Nitsche MA, Paulus W (2003) Manipulation of phosphene thresholds by transcranial direct current stimulation in man. *Exp Brain Res* 150: 375–378.
10. Fregni F, et al. (2005) Anodal transcranial direct current stimulation of prefrontal cortex enhances working memory. *Exp Brain Res* 166:23–30.
11. Dieckhöfer A, et al. (2006) Transcranial direct current stimulation applied over the somatosensory cortex: Differential effect on low and high frequency SEPs. *Clin Neurophysiol* 117:2221–2227.
12. Hummel F, et al. (2005) Effects of non-invasive cortical stimulation on skilled motor function in chronic stroke. *Brain* 128:490–499.
13. Fregni F, et al. (2006) A sham-controlled, phase II trial of transcranial direct current stimulation for the treatment of central pain in traumatic spinal cord injury. *Pain* 122: 197–209.
14. Fregni F, et al. (2006) Treatment of major depression with transcranial direct current stimulation. *Bipolar Disord* 8:203–204.
15. Nitsche MA, et al. (2008) Transcranial direct current stimulation: State of the art, 2008. *Brain Stimulat* 1:206–223.
16. Rogalewski A, Breitenstein C, Nitsche MA, Paulus W, Knecht S (2004) Transcranial direct current stimulation disrupts tactile perception. *Eur J Neurosci* 20:313–316.
17. Leal-Campanario R, Delgado-García JM, Gruart A (2006) Microstimulation of the somatosensory cortex can substitute for vibrissa stimulation during Pavlovian conditioning. *Proc Natl Acad Sci USA* 103:10052–10057.
18. Gruart A, Schreurs BG, del Toro ED, Delgado-García JM (2000) Kinetic and frequency-domain properties of reflex and conditioned eyelid responses in the rabbit. *J Neurophysiol* 83:836–852.
19. Thompson RF (2005) In search of memory traces. *Annu Rev Psychol* 56:1–23.
20. Aou S, Woody CD, Birt D (1992) Increases in excitability of neurons of the motor cortex of cats after rapid acquisition of eye blink conditioning. *J Neurosci* 12:560–569.
21. Weible AP, Weiss C, Disterhoft JF (2003) Activity profiles of single neurons in caudal anterior cingulate cortex during trace eyeblink conditioning in the rabbit. *J Neurophysiol* 90:599–612.
22. Castro-Alamancos MA (2004) Dynamics of sensory thalamocortical synaptic networks during information processing states. *Prog Neurobiol* 74:213–247.
23. Zucker RS, Regehr WG (2002) Short-term synaptic plasticity. *Annu Rev Physiol* 64: 355–405.
24. Izumi Y, Zorumski CF (2008) Direct cortical inputs erase long-term potentiation at Schaffer collateral synapses. *J Neurosci* 28:9557–9563.
25. Liang YC, Huang CC, Hsu KS (2008) A role of p38 mitogen-activated protein kinase in adenosine $A_1$ receptor-mediated synaptic depotentiation in area CA1 of the rat hippocampus. *Mol Brain* 1:13.
26. Bikson M, et al. (2004) Effects of uniform extracellular DC electric fields on excitability in rat hippocampal slices in vitro. *J Physiol* 557:175–190.
27. Fritsch B, et al. (2010) Direct current stimulation promotes BDNF-dependent synaptic plasticity: Potential implications for motor learning. *Neuron* 66:198–204.
28. Kabakov AY, Muller PA, Pascual-Leone A, Jensen FE, Rotenberg A (2012) Contribution of axonal orientation to pathway-dependent modulation of excitatory transmission by direct current stimulation in isolated rat hippocampus. *J Neurophysiol*, 10.1152/jm.00715.2011.
29. Cambiaghi M, et al. (2010) Brain transcranial direct current stimulation modulates motor excitability in mice. *Eur J Neurosci* 31:704–709.
30. Cambiaghi M, et al. (2011) Flash visual evoked potentials in mice can be modulated by transcranial direct current stimulation. *Neuroscience* 185:161–165.
31. Liebetanz D, et al. (2009) Safety limits of cathodal transcranial direct current stimulation in rats. *Clin Neurophysiol* 120:1161–1167.
32. Dockery CA, Liebetanz D, Birbaumer N, Malinowska M, Wesierska MJ (2011) Cumulative benefits of frontal transcranial direct current stimulation on visuospatial working memory training and skill learning in rats. *Neurobiol Learn Mem* 96:452–460.
33. Wachter D, et al. (2011) Transcranial direct current stimulation induces polarity-specific changes of cortical blood perfusion in the rat. *Exp Neurol* 227:322–327.
34. Liebetanz D, et al. (2006) After-effects of transcranial direct current stimulation (tDCS) on cortical spreading depression. *Neurosci Lett* 398:85–90.
35. Liebetanz D, et al. (2006) Anticonvulsant effects of transcranial direct-current stimulation (tDCS) in the rat cortical ramp model of focal epilepsy. *Epilepsia* 47: 1216–1224.
36. Kamida T, et al. (2011) Transcranial direct current stimulation decreases convulsions and spatial memory deficits following pilocarpine-induced status epilepticus in immature rats. *Behav Brain Res* 217:99–103.
37. Nitsche MA, Paulus W (2001) Sustained excitability elevations induced by transcranial DC motor cortex stimulation in humans. *Neurology* 57:1899–1901.
38. Lang N, et al. (2005) How does transcranial DC stimulation of the primary motor cortex alter regional neuronal activity in the human brain? *Eur J Neurosci* 22:495–504.
39. Nitsche MA, et al. (2005) Modulating parameters of excitability during and after transcranial direct current stimulation of the human motor cortex. *J Physiol* 568: 291–303.
40. Furubayashi T, et al. (2008) Short and long duration transcranial direct current stimulation (tDCS) over the human hand motor area. *Exp Brain Res* 185:279–286.
41. Ragert P, Vandermeeren Y, Camus M, Cohen LG (2008) Improvement of spatial tactile acuity by transcranial direct current stimulation. *Clin Neurophysiol* 119:805–811.
42. Antal A, Nitsche MA, Paulus W (2001) External modulation of visual perception in humans. *Neuroreport* 12:3553–3555.
43. Antal A, et al. (2004) Direct current stimulation over V5 enhances visuomotor coordination by improving motion perception in humans. *J Cogn Neurosci* 16:521–527.
44. Antal A, et al. (2008) Transcranial direct current stimulation over somatosensory cortex decreases experimentally induced acute pain perception. *Clin J Pain* 24:56–63.
45. Stagg CJ, Nitsche MA (2011) Physiological basis of transcranial direct current stimulation. *Neuroscientist* 17:37–53.
46. Nitsche MA, et al. (2003) Pharmacological modulation of cortical excitability shifts induced by transcranial direct current stimulation in humans. *J Physiol* 553:293–301.
47. Nitsche MA, et al. (2004) Catecholaminergic consolidation of motor cortical neuroplasticity in humans. *Cereb Cortex* 14:1240–1245.
48. Islam N, et al. (1995) c-Fos expression mediated by N-methyl-D-aspartate receptors following anodal polarization in the rat brain. *Exp Neurol* 133:25–31.
49. Huang CC, Liang YC, Hsu KS (1999) A role for extracellular adenosine in time-dependent reversal of long-term potentiation by low-frequency stimulation at hippocampal CA1 synapses. *J Neurosci* 19:9728–9738.
50. van Calker D, Müller M, Hamprecht B (1979) Adenosine regulates, via two different types of receptors, the accumulation of cyclic AMP in cultured brain cells. *J Neurochem* 33:999–1005.
51. Miranda PC, Lomarev M, Hallett M (2006) Modeling the current distribution during transcranial direct current stimulation. *Clin Neurophysiol* 117:1623–1629.
52. Girgis M, Shih-Chang W (1981) *A New Stereotaxic Atlas of the Rabbit Brain* (Warren H. Green, St. Louis).